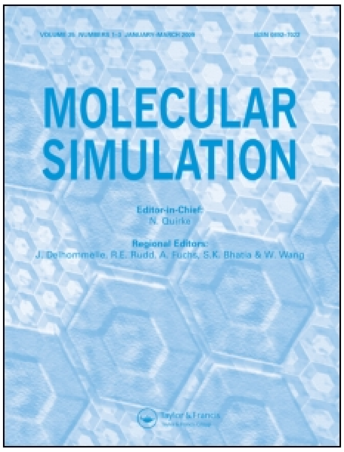

Molecular Simulation
Publication details, including instructions for authors and subscription information:
http://www.informaworld.com/smpp/title~content=t713644482

Computer Simulations in Zeolite Catalysis Research

C. J. J. Den Ouden[a]; B. Smit[a]; A. F. H. Wielers[a]; R. A. Jackson[b]; A. K. Nowak[c]
[a] Koninklijke/Shell Laboratorium Amsterdam (Shell Research B.V.), Amsterdam, The Netherlands [b] Department of Chemistry, University of Keele, Keele, Staffordshire, UK [c] Davy Faraday Laboratory, The Royal Institution, London, UK

To cite this Article Ouden, C. J. J. Den , Smit, B. , Wielers, A. F. H. , Jackson, R. A. and Nowak, A. K.(1989) 'Computer Simulations in Zeolite Catalysis Research', Molecular Simulation, 4: 1, 121 — 136
To link to this Article: DOI: 10.1080/08927028908021969
URL: http://dx.doi.org/10.1080/08927028908021969

Molecular Simulation, 1989, Vol. 4, pp. 121–136
Reprints available directly from the publisher
Photocopying permitted by license only

COMPUTER SIMULATIONS IN ZEOLITE CATALYSIS RESEARCH

C.J.J. DEN OUDEN[1], B. SMIT[1], A.F.H. WIELERS[1], R.A. JACKSON[2], and A.K. NOWAK[3]

[1] *Koninklijke/Shell Laboratorium Amsterdam (Shell Research B.V.), Badhuisweg 3, 1031 CM Amsterdam, The Netherlands*
[2] *Department of Chemistry, University of Keele, Keele, Staffordshire, ST5 5BG, UK*
[3] *Davy Faraday Laboratory, The Royal Institution, 21 Albemarle Street, London W1X 4BS, UK*

(*Received January 1989, accepted February 1989*)

An overview is presented of computer simulations applied to zeolite catalysis research. It is shown that using (numerical) statistical methods one is able to explain features observed in Ni^{2+} ion exchange. Lattice energy minimisation calculations confirm the validity of the model used. Furthermore, Monte Carlo and molecular dynamics simulations offer opportunities to describe adsorption and mass transport phenomena at a molecular level which is of importance in studies on shape selective catalysis.

KEY WORDS: Zeolites, catalysis, Monte Carlo, molecular dynamics, adsorption, mass transport

INTRODUCTION

Zeolites are microporous crystalline materials consisting of silicon, aluminium, oxygen and exchangeable charge compensating extra framework cations. The framework is built up by interlinking TO_4 tetrahedra (in which the T-sites are occupied by either silicon or aluminium). The zeolite framework chemical composition is indicated by the Al/Si ratio. Loewenstein's rule [1] forbids Al–O–Al sequences in the lattice and hence the Al/Si ratio lies between 0 (siliceous zeolites such as silicalite) and 1 (high alumina zeolites such as zeolite X and A). Zeolites containing H^+ ions as charge compensating cations can act like solid acids, the acidity primarily depending on the aluminium content in the zeolite lattice [2], and are used as acidic catalysts in various hydrocarbon conversion reactions.

The catalytic performance of zeolities can be modified by introducing various cations via ion exchange procedures. In particular, transition metal ions present in the micropores may act as alternative catalytic centres in reactions other than those requiring carbenium ions as intermediates [3]. Because of the catalytic properties exhibited, zeolites are widely used as components in heterogeneous catalysts in the oil- and chemical processing industries [4, 5].

For zeolites, catalytic selectivity is not only a matter of stoichiometry, but also steric constraints for molecular transport in the zeolitic void space can be the reason for the so called shape selectivity [6]. Shape selectivity can in principle be obtained by adjusting the size [7] and accessibility [8] of the micropores. A distinction is made between three types of shape selectivity depending on whether the pore size limits the entrance of the reacting molecule (reactant selectivity), the departure of the product

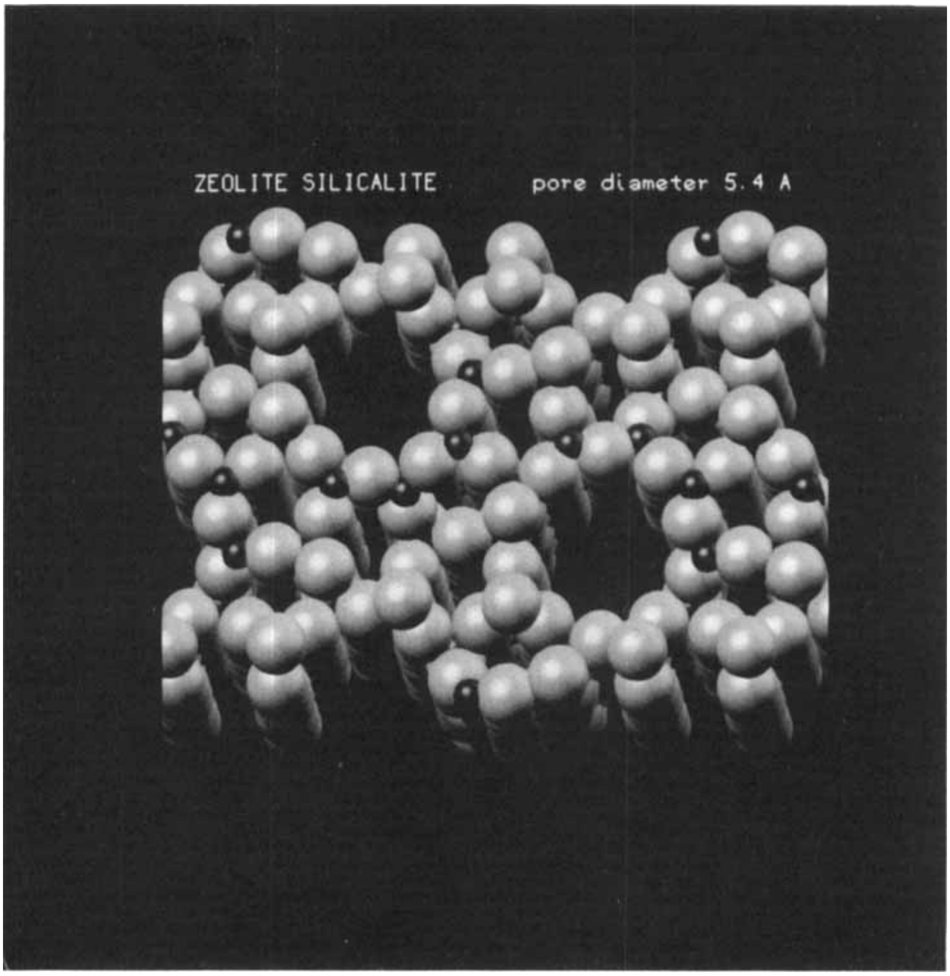

Figure 1 Structure of zeolite silicalite (all silica form of ZSM-5). The channel system consists of two types of channels: straight channels (viewed) and sinusoidal channels (not visible) perpendicular to the straight channels. The pore diameter is 5.4 Å. Oxygen atoms are coloured yellow, T-sites (silicon or aluminium atoms) are tetrahedrally surrounded by oxygen atoms and are coloured red. (See colour plate V.)

molecule (product selectivity) or the formation of certain transition states along the reaction coordinate (restricted transition state selectivity).

In this paper, we present an overview of computer simulation methods which might be of use in the field of zeolite catalyst modification and characterisation. In addition, techniques used in the description of molecular transport phenomena and adsorption in zeolites are discussed.

The systems considered in the section on modification and characterisation part are Ni^{2+} exchanged mordenite and ZSM-5 materials which are used as olefin oligomerisation catalysts [9]. Examples of molecular transport and adsorption considered are methane diffusion and adsorption in the zeolites silicalite (which is the siliceous form

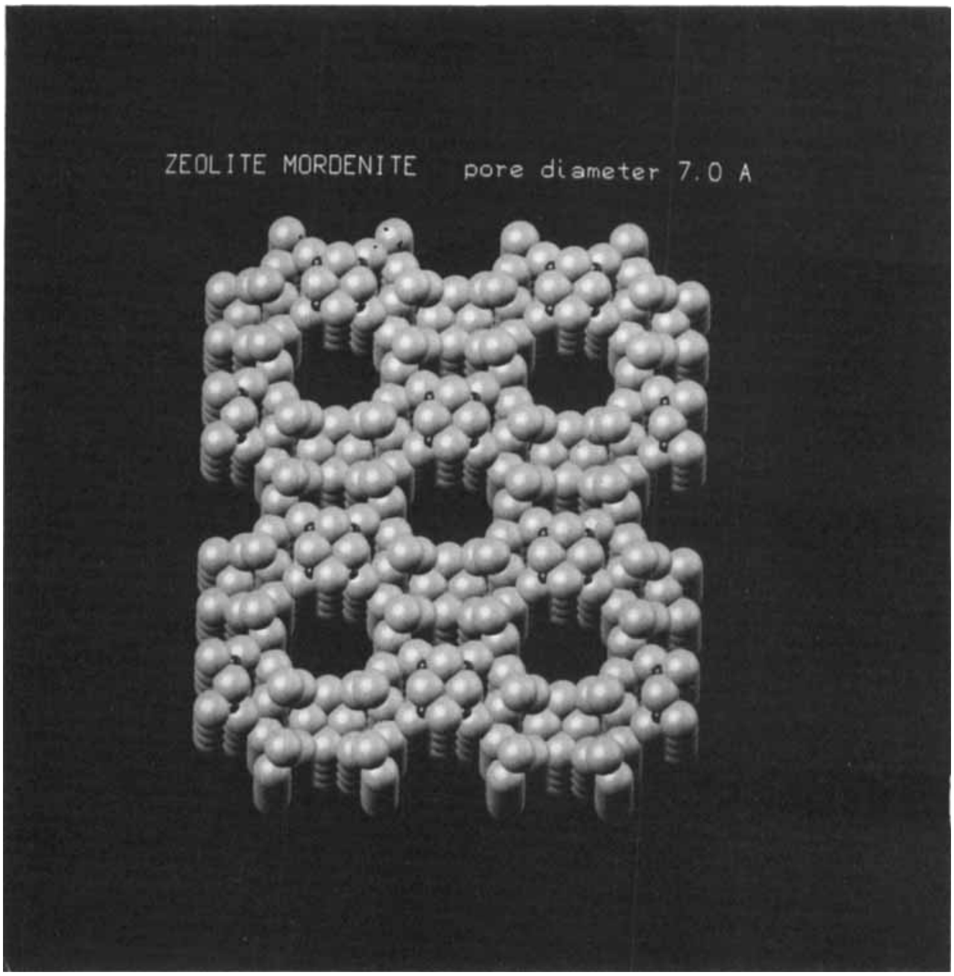

Figure 2 Structure of zeolite mordenite. The channel system consists of two types of channels which are parallel to each other (both viewed), the main channel has a pore diameter of 7 Å, whereas the secondary channel is much smaller. Side pockets are located at the edges of the main channels and are small cages with an entrance diameter of approximately 5 Å. Oxygen atoms are coloured yellow, T-sites (silicon or aluminium atoms) are tetrahedrally surrounded by oxygen atoms and are coloured red. (See colour plate VI.)

of ZSM-5) and mordenite. Structural information on various types of zeolites are presented in Figure 1, 2, and 3.

ZEOLITE CATALYST MODIFICATION AND CHARACTERISATION

The ion exchange properties of zeolites make it possible to modify and to tune the catalytic performance by introducing different cations in the micropores. Therefore, ion exchange studies are important both from a practical and a fundamental point of

Figure 1 Structure of zeolite silicalite (all silica form of ZSM-5). The channel system consists of two types of channels: straight channels (viewed) and sinusoidal channels (not visible) perpendicular to the straight channels. The pore diameter is 5.4 Å. Oxygen atoms are coloured yellow, T-sites (silicon or aluminium atoms) are tetrahedrally surrounded by oxygen atoms and are coloured red. (See colour plate VII.)

view. It is generally accepted that the exchange capacity of zeolites is related to the amount of aluminium in the zeolite lattice. This feature stems from the fact that an aluminium atom substituted for a silicon atom in the lattice causes an excess negative charge. This negative charge is compensated for by the presence of an extra framework cation. Recently however, we showed that the exchange of monovalent cations for divalent cations, such as Ni^{2+}, is not a simple stoichiometric one, especially for low aluminium concentrations in the zeolite.Furthermore the amount of Ni^{2+} that can be exchanged is related to the distribution of aluminium in the zeolite lattice [10].

Several research groups [11, 12] have also investigated exchange properties of both mono- and divalent metal ions in siliceous ($Al/Si < 0.05$) zeolites. Whereas monovalent ions generally reveal complete exchange ($M^+/Al = 1$), the ion exchange properties for divalent metal ions are less clear cut and in general an incomplete exchange is found, i.e. $M^{2+}/Al < 0.5$.

The location of divalent cations (and hence the location of the catalytic centres) inside zeolites is still a matter of extensive debate. With high alumina zeolites, the concentration of divalent cations attainable is in general sufficiently high to allow determination of their location by standard XRD techniques [13, 14], but with siliceous zeolites, levels of exchange are too low to allow investigation of the location of divalent cations by these methods.

In order to explain and understand the peculiar exchange properties of divalent cations in siliceous ZSM-5, we have developed two statistical models, one based on basic statistics and one based on a Monte Carlo numerical statistical model respectively [10]. The concept of both models is the same and is based on a random distribution of aluminium atoms in the zeolite lattice. Ni^{2+} ions are assumed to coordinate to Al–O–Si–O–Al sequences in the framework, thus the amount of Ni^{2+} which can be incorporated equals the number of Al–O–Si–O–Al sequences found. In the first model (which will be referred to as the analytical or AN model), we derived a simple analytical expression from basic statistics which relates the Ni/Al ratio to the ZSM-5 Al/Si ratio [10]:

$$\mathrm{Ni/Al} = 5.96\ \mathrm{Al/Si} \tag{1}$$

This analytical expression can only be obtained if Loewenstein's rule is neglected which is only allowed in situations dealing with low aluminium contents (as is the case in this paper). If one wishes to include Loewenstein's rule, the statistics become much more complicated. In order to obey Loewenstein's rule, we additionally employed a Monte Carlo numerical method (referred to as the MC method) in which loewenstein's rule can easily be implemented. For this purpose we have calculated the number of Al–O–Si–O–Al sequences in a ZSM-5 crystallite consisting of $3 \times 3 \times 3 = 27$ unit cells. Periodic conditions have been used to overcome boundary effects.

The MC procedure involves the generation of an ensemble of N_{MC} ZSM-5 crystallites. In each of these crystallites, N_{Al} aluminium atoms are randomly distributed over the available T-sites in the crystallite. N_{Al} depends on the Al/Si ratio considered. Crystallites in the ensemble which violate Loewenstein's rule are rejected from the ensemble, thus reducing the number of crystallites from N_{MC} to N^*_{MC}. Typical values for N^*_{MC} are of the order of 200,000. The total number of Al–O–Si–O–Al sequences is counted from the reduced ensemble of crystallites. Following this procedure, the average number of Al–O–Si–O–Al sequneces, $N_{Al\text{-}O\text{-}Si\text{-}O\text{-}Al}$, and thus the average number of Ni^{2+} ions per crystallite, N_{Ni}, is given by:

$$N_{Ni} = N_{Al\text{-}O\text{-}Si\text{-}O\text{-}Al}/N^*_{MC} \tag{2}$$

and therefore:

$$\mathrm{Ni/Al} = N_{Al\text{-}O\text{-}Si\text{-}O\text{-}Al}/\,(N^*_{MC} \cdot N_{Al}) \tag{3}$$

Figure 4 displays the Ni/Al ratio versus the ZSM-5 Al/Si ratio as obtained from chemical analysis (experimental), the AN method and the MC method.

The excellent agreement between modelling results and experimental data is striking, indicating that aluminium is indeed randomly distributed in siliceous ZSM-5 and

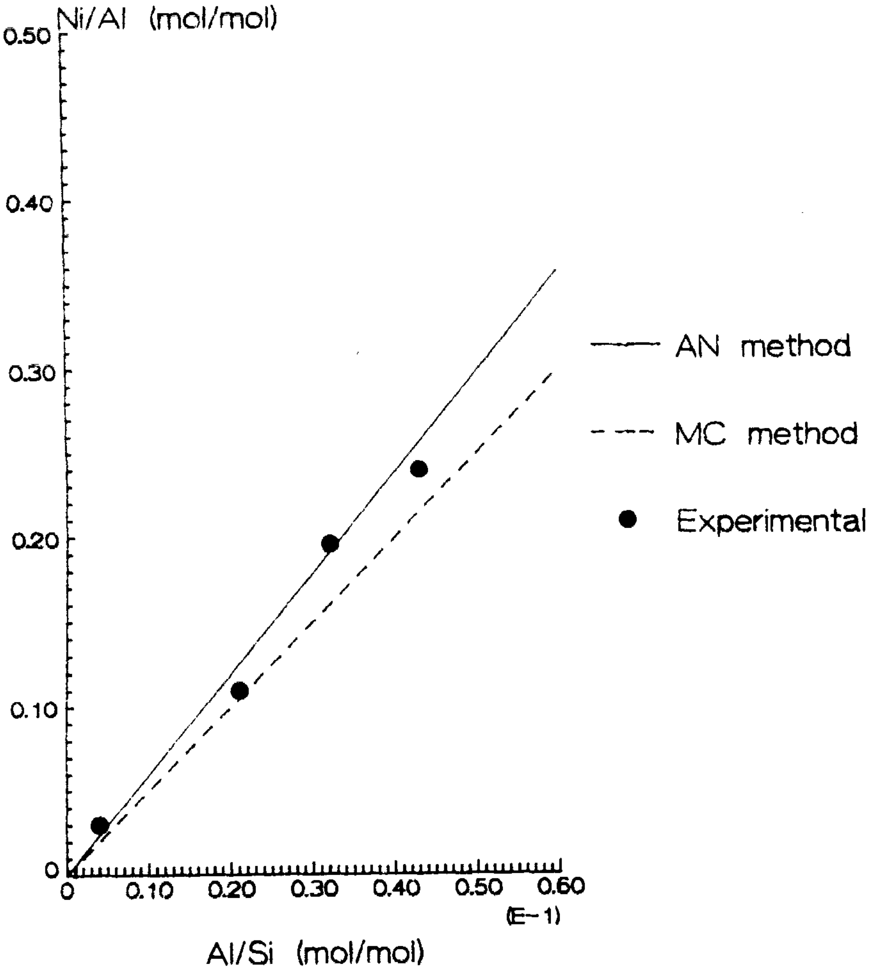

Figure 4 Ni/Al molar ratio versus Al/Si molar ratio according to the analytical (AN), and the Monte Carlo (MC) procedure. Experimental values are represented by the solid dots.

that Ni^{2+} ions are coordinated to the ZSM-5 lattice via specific Al-O-Si-O-Al sequences. From Figure 4, it can also be concluded that neglecting Loewenstein's rule (AN-method) for low aluminium contents (as is the case in this paper) is justified. Systems with higher Al/Si ratios are under investigation, and we expect that in these cases Loewenstein's rule has to be incorporated (i.e. the MC-method should give better results in this case).

In order to verify our model and to unravel the location of Ni^{2+} ions in high silica mordenite, we followed an alternative computational approach [15] based on lattice energy minimisation calculations which already proved to be valuable techniques in simulation studies on zeolite structures [16] and the determination of zeolite framework stabilities [17]. Various Al-O-(Si-O)$_N$-Al framework sequences (with $N > 0$ to obey Loewenstein's rule) were investigated. For Ni^{2+} ions, three different locations in the mordenite structure can be distinguished: in the12-ring main channel, the 8-ring

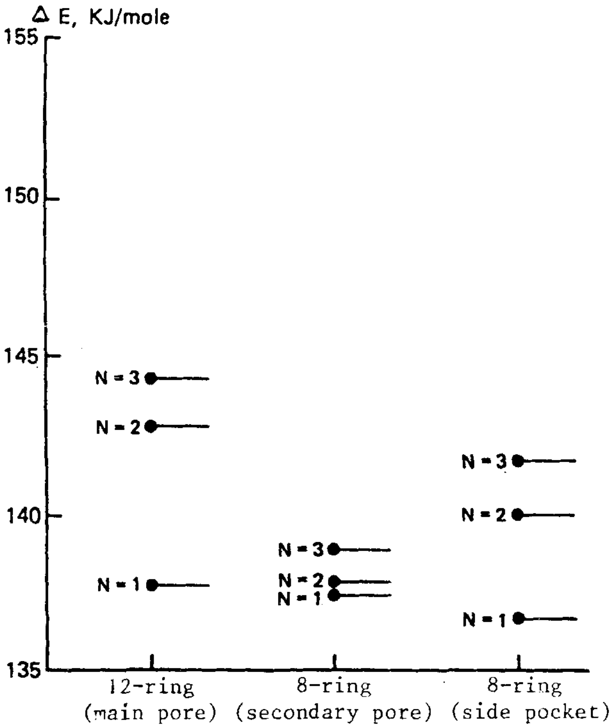

Figure 5 Mordenite framework stability as a function of the location of the Ni^{2+} ion and framework $Al-O-(Si-O)_N-Al$ sequence. ΔE is the difference between the all silica mordenite lattice energy and the Ni-alumino mordenite lattice energy. Decreasing ΔE means increasing coordination strength.

secondary channel and the 8-ring side pockets at the edges of the main channels. The results for the various locations and the various values of N are displayed in Figure 5.

As can clearly be seen from Figure 5, Ni^{2+} is preferentially coordinated to an Al-O-Si-O-Al ($N = 1$) sequence. The energy gaps between the levels $N = 1$ and $N = 2$ for the case of location in the 12-ring main channel and 8-ring side-pocket are substantial whereas this energy gap is much less pronounced for Ni^{2+} located in the 8-ring secondary channels.

The main conclusion which can be drawn from the modification and characterisation modelling studies on Ni-alumino ZSM-5 and mordenite is that there is strong evidence that Ni^{2+} is coordinated to the zeolite lattice via specific $Al-O-(Si-O)_N-Al$ sequences, preferentially with $N = 1$. Furthermore, these studies enable us to relate the amount of Ni^{2+} to be incorporated to the aluminium distribution throughout the framework.

ADSORPTION AND DIFFUSION IN ZEOLITE CATALYSTS

In order to understand the high selectivities observed in adsorption processes and catalytic conversions of hydrocarbons over zeolite catalysts, it is necessary to study the behaviour of molecules inside the micropores of a zeolite. Since this kind of information is difficult to obtain from direct experiments, computer simulations might offer valuable alternative approaches to the problem.

In this section, we will show an example in which Monte Carlo simulations of methane adsorption in mordenite predict a very peculiar adsorption behaviour at various Al/Si ratios [18]. Furthermore, we will present molecular dynamics simulations on molecular mass transport phenomena for methane migrating in the micropores of siliceous mordenite and silicalite [19].

Adsorption

Following the methods pioneered by Yashonath *et al.* [20], we have carried out Monte Carlo adsorption simulations at low coverage of methane. This allows us to ignore methane-methane interactions and hence only methane-zeolite interactions are taken into account. The potentials are taken from Kiselev *et al.* [21] and Yashonath *et al.* [20].

The Monte Carlo calculations were performed on a Cray XMP/18 computer using the conventional Metropolis algorithm [22]. A methane molecule is initially placed inside a micropore. One Monte Carlo step consists of two parts: first a random displacement of the centre of mass followed by an arbitrary rotation of the entire molecule. In order to eliminate the effect of boundaries, periodic conditions have been used with a period equal to one zeolite unit cell.

In our model, we assume that methane has the same interaction with silicon and aluminium atoms in the zeolite, thus silicon and aluminium are treated as equivalent T-sites. However, as the Al/Si ratio is increased, the positive charge on the zeolite lattice decreases. This decrease is compensated by sodium ions at extra framework positions [23].

In Figure 6, the calculated adsorption enthalpy of methane in mordenite is presented as a function of the Al/Si ratio at 300 K. A sudden decrease of the adsorption enthalpy is observed as the Al/Si ratio exceeds 0.15.

The distribution of positions occupied by methane in mordenite are shown in Figure 7. At low Al/Si ratios (Figure 7a), one sees that methane is located in the straight channels and in the side pockets. The colour coding in figure 7a shows that methane located in such a side pocket has a considerably lower energy than a methane molecule in the central channel. As the Al/Si ratio is increased, the side pockets are effectively blocked by the sodium ions (Figure 7b). In this case, methane cannot reach these low energy sites anymore. We suggest that this effective blocking by the sodium ions explains the observed decrease of the adsorption enthalpy at high Al/Si ratios (cf. Figure 6). Work is in progress in order to obtain experimental verification of our observations.

Also displayed in Figure 6 is the experimental adsorption enthalpy for methane in mordenite at Al/Si = 0.09 [27]. It is clearly seen that the agreement between calculated and experimental adsorption enthalpies is very good, indicating the strength of the method.

In this study, we have restricted ourselves to the special case of methane in mordenite. This relatively simple case clearly illustrates how computer simulations can provide microscopic information about the arrangement and pore accessibilities of molecules in zeolites and how this information may help us to predict the behaviour

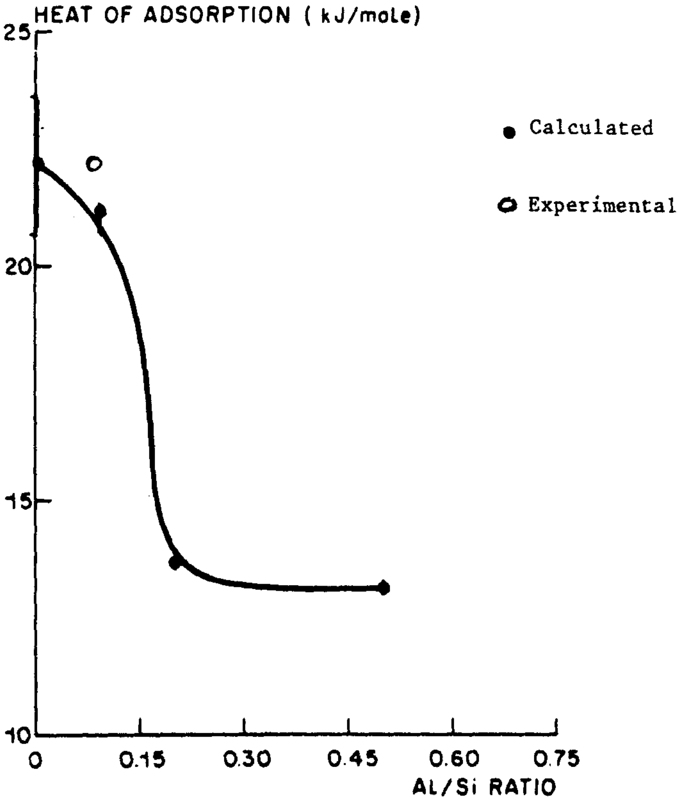

Figure 6 Adsorption enthalpy of methane in mordenite as a function of the Al/Si ratio (T = 300 K).

of such zeolites.

Diffusion

Methane diffusion in siliceous mordenite and silicalite (siliceous ZSM-5) was simulated using molecular dynamics procedures. The methane-zeolite and methane-methane interaction potentials were obtained from reference 21.

The molecular dynamics simulations were carried out on a Cray XMP/18 computer under NVT conditions (constant number of particles, constant volume, constant temperature) using the Verlet algorithm [24]. Each time step, the temperature, T_c, of the ensemble of adsorbed methane molecules was calculated followed by a scaling of the velocities to the desired simulation temperature T_w:

$$V_i \rightarrow \sqrt{\frac{T_w}{T_c}}\, V_i \tag{4}$$

The time step length, δt, was typically of the order of 10^{-3} ps. Total simulation times varied from a few ps up to 100 ps. The simulations were carried out in a volume of $2 \times 2 \times 2 = 8$ unit cells taking periodic boundary conditions into account. The

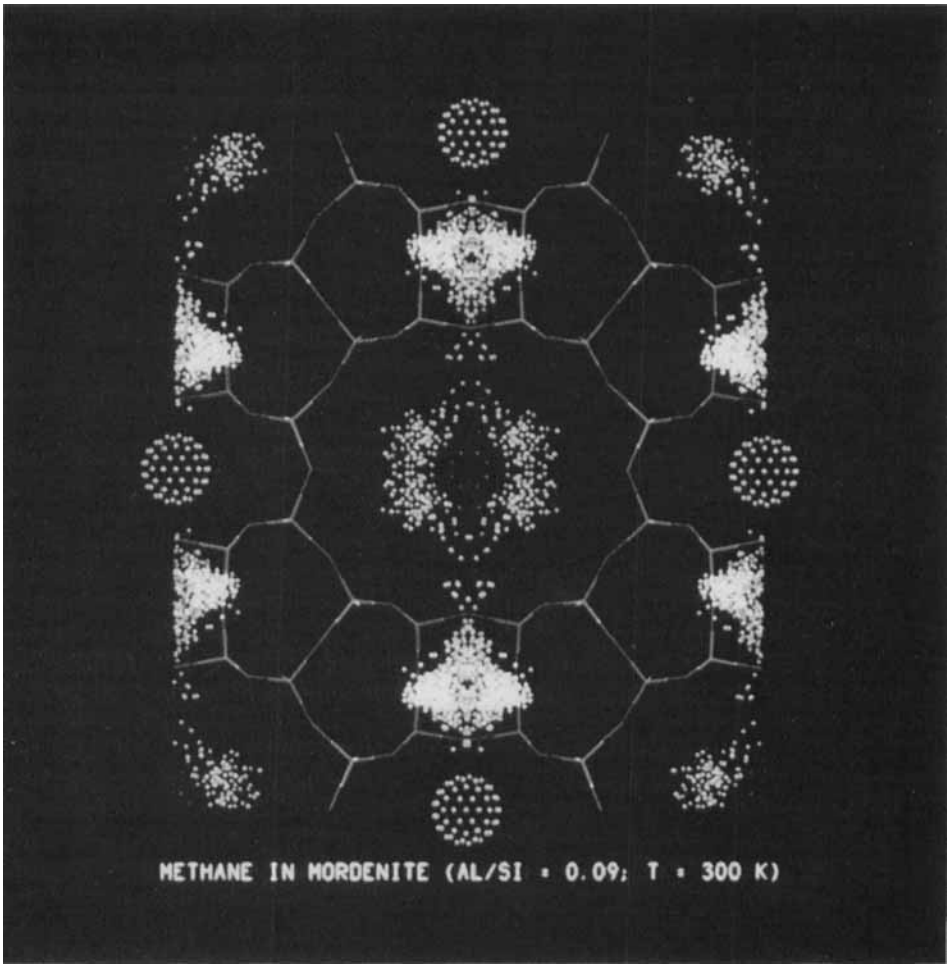

Figure 7a Distribution of methane adsorbed in mordenite at 300 K and Al/Si = 0.09. The zeolite structure is represented by oxygen (red rods), aluminium and silicon (blue rods) and extra-framework sodium ions (green spheres). Each spot inside the mordenite pore represents the projection of the centre of mass of the methane molecule. The colour of the spot is a measure for the energy of the methane molecule (the energy decreases in the order red, yellow, green, green/white). (See colour plate VIII.)

maximum zeolite loading was 4 and 3 methane molecules per unit cell silicalite and mordenite, respectively. So the total number of methane molecules in these cases equals 32 for silicalite and 24 for mordenite. The diffusion coefficient was obtained from the mean squared displacements of the methane molecules. Diffusivities of methane migrating in silicalite and siliceous mordenite have been calculated as a function of zeolite loading. Figure 8 displays the results obtained at T = 300 K.

Although the scatter in Figure 8 is substantial, it is clearly seen that the diffusivity of methane in silicalite is almost independent of the zeolite loading whereas the

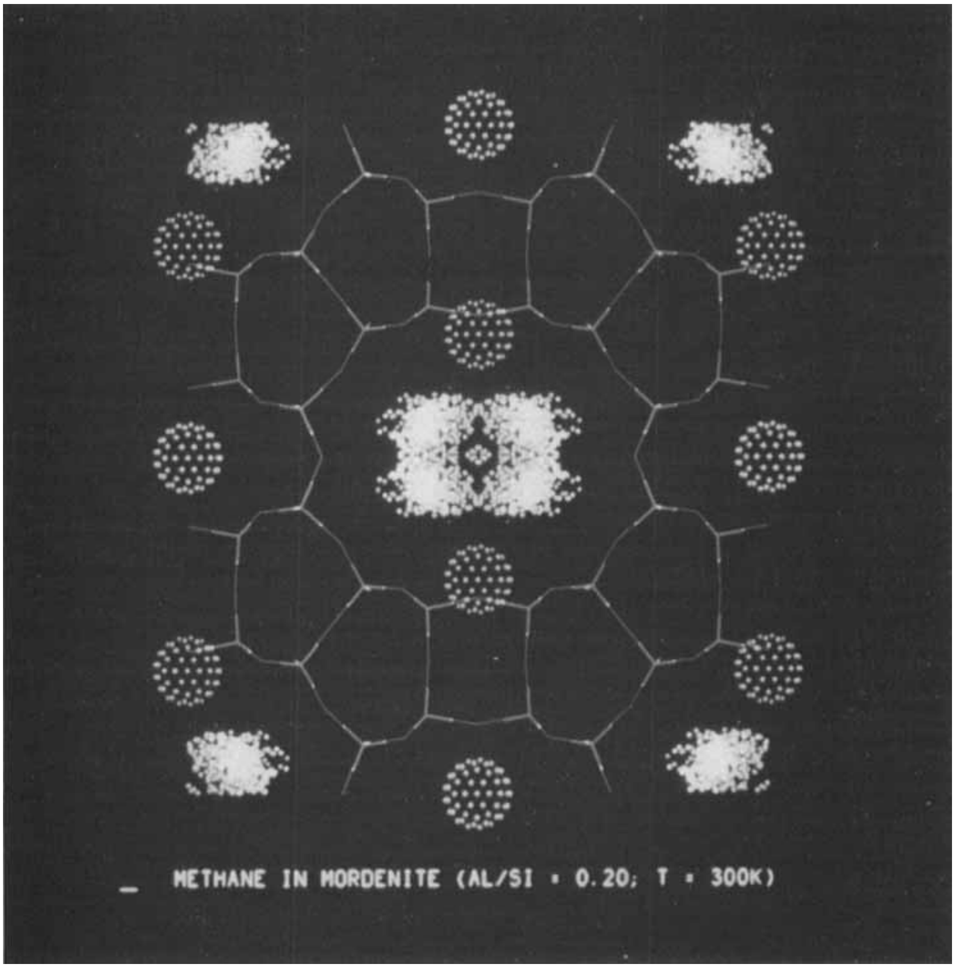

Figure 7b Distribution of methane adsorbed in mordenite at 300 K and Al/Si = 0.2. The zeolite structure is represented by oxygen (red rods), aluminium and silicon (blue rods) and extra-framework sodium ions (green spheres). Each spot inside the mordenite pore represents the projection of the centre of mass of the methane molecule. The colour of the spot is a measure for the energy of the methane molecule (the energy decreases in the order red, yellow, green, green/white). (See colour plate IX.)

diffusivity of methane in mordenite seems to be strongly dependent on the zeolite loading. This feature can be explained by considering Figure 9a. This figure shows the trajectory of one methane molecule in mordenite over a period of 100 ps. Obviously, a substantial part of this time the methane molecule is sited in an 8-ring side pocket where its mobility and interaction energy is very low. It can be envisaged that on increasing the loading, the side pockets are gradually filled with methane molecules. This leaves only the 12-ring main channel open for diffusion for the remaining methane molecules and hence results in a higher value of the diffusion coefficient because of the absence of (empty) side pockets.

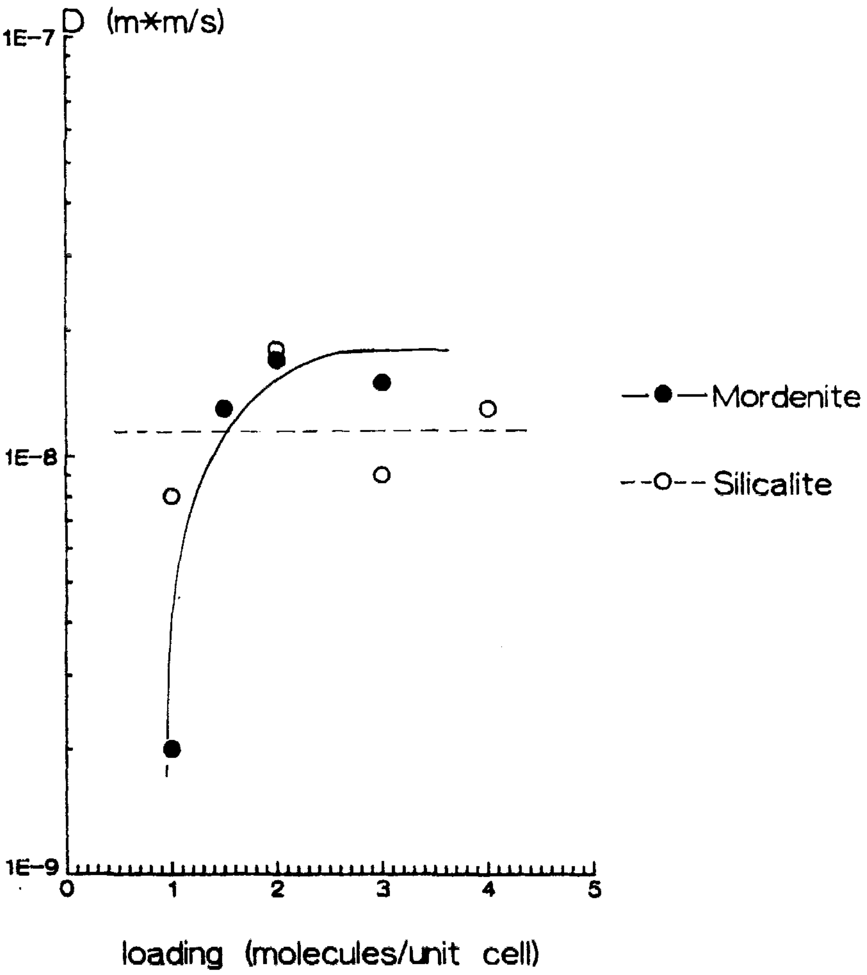

Figure 8 Diffusion coefficient (m^2 s) versus zeolite loading for methane migrating in all silica mordenite and silicalite at T = 300 K.

Table 1 Experimental and calculated diffusion coefficients for methane in all silica mordenite and silicalite.

method	*T* (*K*)	*silicalite* (*D* × *10*^{8} *m*^{2}/*s*)	*mordenite* (*D* × *10*^{8} *m*^{2}/*s*)
Membrane diffusion measurements (ref. 25)	334	0.011	–
PFG-NMR (ref. 26)	300	1.1	–
Molecular dynamics	300	1.2	1.8

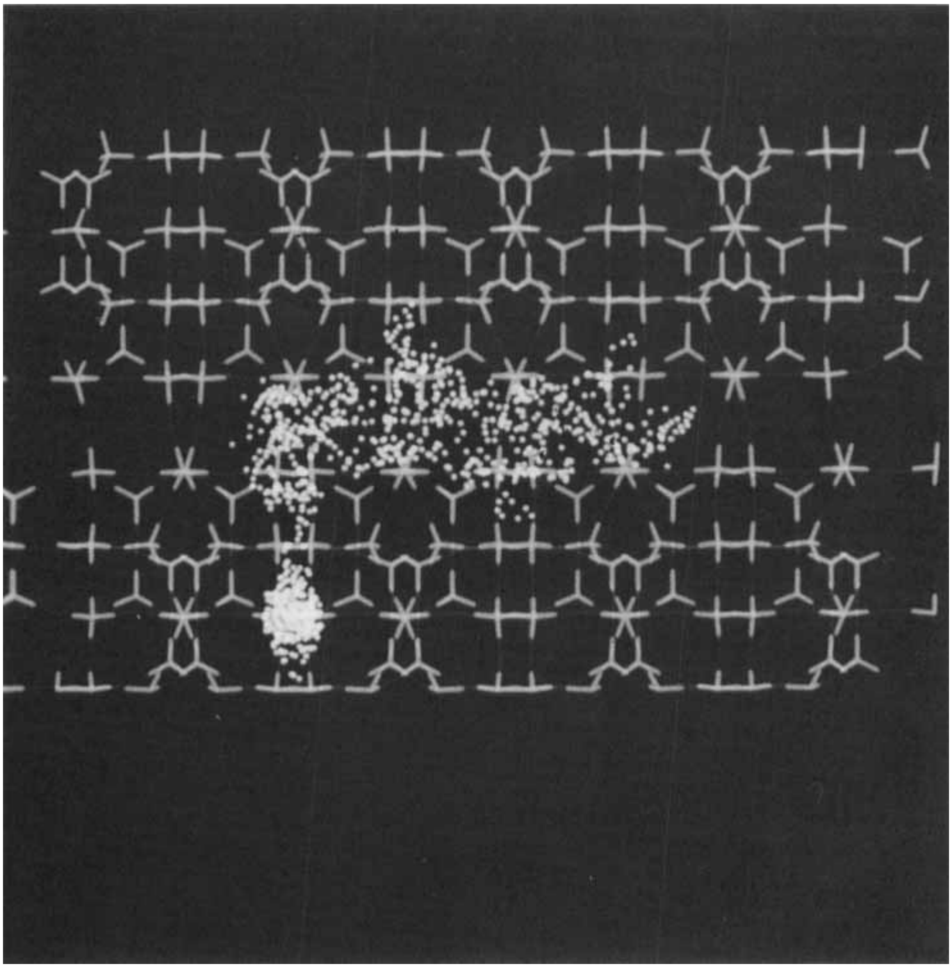

Figure 9a Trajectory of a methane molecule migrating in the main channel of mordenite (the main channel is horizontally displayed) over a time period of 100 ps. The simulation temperature equals 300 K. Each spot inside the micropores represents the projection of the centre of mass of the methane molecule. (See colour plate X.)

Figure 9b displays the trajectory of one methane molecule migrating in silicalite over a 100 ps. time period. An interesting feature in this figure is the difference in residence times of the methane molecule localised in the straight (horizontal in Figure 9b) and sinusoidal (vertical in Figure 9b) channels of the silicalite pore system. It is clearly seen that residence times for methane adsorbed in the sinusoidal channels are longer (high density of dots) than the residence times in the straight channels (low density of dots).

Calculated diffusion coefficients for methane self diffusion in silicalite and siliceous mordenite are represented in table I. Furthermore, experimental diffusion coefficients

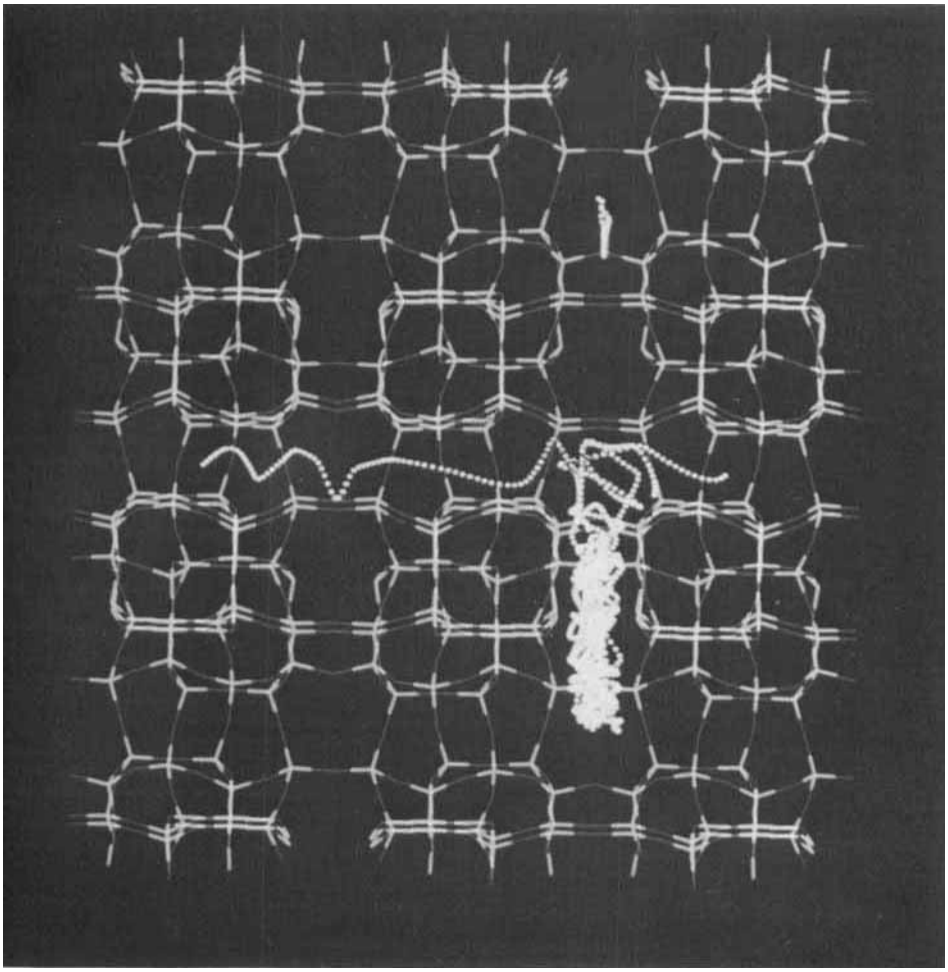

Figure 9b Trajectory of a methane molecule migrating in the straight and sinusoidal channel of silicalite (the straight channel is horizontally displayed whereas the sinusoidal channel is vertically displayed) over a time period of 100 ps. The simulation temperature equals 300 K. Each spot inside the micropores represents the projection of the centre of mass of the methane molecule. (See colour plate XI.)

obtained via membrane diffusion measurements [25] and Pulse Field Gradient (PFG) NMR techniques [26] are also represented for comparison. To our knowledge, no experimental data for methane diffusion in siliceous mordenite is available.

From table I, we see very good agreement between molecular dynamics results and results obtained via PFG-NMR experiments. The difference in the diffusion coefficients obtained via uptake measurements and NMR spectroscopy has often been observed in the literature and is still a matter of much controversy. However, we stress that self diffusion is measured by PFG-NMR whereas uptake measurements consider diffusion caused by concentration gradients. Molecular dynamics simulates self diffusion, so agreement with PFG-NMR would seem logical.

CONCLUSIONS

This paper has highlighted some examples of computer simulations applied to zeolite catalysis research. Although the systems under study are to some extent simplified, the characteristics and the strength of the methods used are clearly demonstrated. It has become clear that the field of applications of computer simulations in combination with experimental work is very wide. We have shown that in two different areas of zeolite catalyst and catalysis research, modification/characterisation and the description of mass transport/adsorption, the latter being related to shape selective catalysis, simulations proved to be powerful techniques. It should be stressed that catalysis research for a long time to come is, and as a matter of fact should be, mainly an experimentally based science. Nevertheless we believe that computer simulations can contribute to a better understanding of zeolite catalysts and catalysis at a molecular level. Such an understanding is crucial for the future design of tailor-made zeolite catalysts with an ultra-high selectivity and activity.

Acknowledgements

We wish to thank many people who have given us assistance with the studies outlined in this paper and in particular D.P. de Bruijn, C.R.A. Catlow, A.K. Cheetham, H.P.C.E. Kuipers, S. Pickett, M.F.M. Post and J.M. Thomas.

References

[1] D.W. Breck "Zeolite Molecular Sieves" Robert E. Krieger Publishing Company, Malabar, Florida (1984)

[2] See e.g. M. Neuber, V. Dondur, H.G. Karge, L. Pacheco, S. Ernst, and J. Weitkamp in "Spectroscopic and catalytic characterisation of faujasites via the $(NH_4)_2SiF_6$ method" Proc. Int. Symp. "Innovation in Zeolite Materials Science", Elsevier, Amsterdam (1988), page 461.

[3] Kh. Minachev and Ya. I. Isakov in J.A. Rabo (Ed.), "Zeolites Chemistry and Catalysis", ACS monograph (1976), volume 171

[4] I.E. Maxwell "Zeolite catalysis in hydrocarbonprocessing technology" *Catalysis Today* **1**(4), 385 (1987).

[5] W.F. Hoelderich "New horizons in catalysis using modified and unmodified pentasil zeolites" *Pure Appl. Chem.*, **58**(10), 1383 (1986)

[6] I.E. Maxwell "Shape selective catalysis and process technology via molecular inclusion in zeolites" *J. Inclusion Phenom.* **4**,1 (1986)

[7] E.F. Vansant "Pore size engineering in zeolites" Proc. Int. Symp. "Innovation in Zeolite Materials Sciene", Elsevier, Amsterdam (1988), page 143

[8] C. Mirodatos and D. Barthomeuf "A new concept in zeolite-catalysed reactions: energy gradient selectivity" *J. of Catalysis*,**93**,246 (1985)

[9] See e.g. G. Wendt, K. Haenau, R. Dimitrova, Z. Popova, and Ch. Dimitrov "Dimerisation of n-butenes on nickel mordenite catalysts" *React. Kinet. Catal. Lett.*, **31**,383 (1986)

[10] C.J.J. den Ouden, A.F.H. Wielers, H.P.C.E. Kuipers, M. Vaarkamp, M. Mackay, and M.F.M. Post "Ion exchange of Ni^{2+} ions in siliceous ZSM-5" Paper to be presented at the 8th Int. Zeolite Conf. Amsterdam (1989)

[11] P. Chu and E.G. Dwyer "Inorganic Cation Exchange properties of zeolite ZSM-5" *ACS, Symp. Ser.*, **218**,59 (1983)

[12] D.P. Matthews and L.V.C. Rees "Ion exchange in ZSM-5 zeolite" *Chem. Age. India*, **37**,(5), 353 (1986)

[13] P.J. Maddox, J. Spachursky, and J.M. Thomas "Probing structural changes during the onset of catalytic activity by in situ X-ray diffractometry" *Cat. Lett.*, **1**,191 (1988)

[14] J.M. Thomas, C. Williams, and T. Rayment "Monitoring cation-site occupancy of nickel-exchanged zeolite Y catalysts by high-temperature in situ X-ray powder diffractometry" *J. Chem. Soc. Faraday Trans.*, **I**, **84**(9), 2915 (1988)

[15] C.J.J. den Ouden, R.A. Jackson, C.R.A. Catlow, and M.F.M. Post "The location of Ni^{2+} ions in siliceous mordenite: a computational approach" To be published

[16] R.A. Jackson and C.R.A. Catlow "Computer simulation studies of zeolite structure" *Molecular Simulation*, **1**,207 (1988)

[17] G. Ooms, R.A. van Santen, C.J.J. den Ouden, R.A. Jackson, and C.R.A. Catlow "Relative stabilities of zeolitic alumino silicates" *J. Phys. Chem.*, **92**,4462 (1988)

[18] B. Smit and C.J.J. den Ouden "Monte Carlo simulations on the relation between structure and properties of zeolites: The adsorption of small hydrocarbons" *J. Phys. Chem.*, **92**,7169 (1988)

[19] To be published

[20] S. Yashonath, J.M. Thomas, A.K. Nowak, and A.K. Cheetham "The siting, energetics and mobility of saturated hydrocarbons inside zeolitic cages: methane in zeolite Y" *Nature*, **331**,601 (1988)

[21] A.V. Kiselev, A.A. Lopatkin, and A.A. Schulga "Molecular statistical calculation of gas adsorption by silicalite" *Zeolites*, **5**,261 (1985)

[22] N. Metropolis, A.W. Rosenbluth, M.N. Rosenbluth, A.H. Teller, and E. Teller "Equation of state calculations by fast computing machines" *J. Chem. Phys.*, **21**,1081 (1953)

[23] W.J. Mortier "Compilation of extra framework sites in zeolites" Butterworth Scientific Limited (1982)

[24] M.P. Allen and D.J. Tildesley "Computer Simulation of Liquids" Clarendon Press, Oxford (1987)

[25] D.T. Hayhurst and A.R. Paravar "Diffusion of C_1 to C_5 normal paraffins in silicalite" *Zeolites*, **8**,27 (1988)

[26] J. Karger, H. Pfeifer, and D. Freude "NMR Investigations of self-diffusion in Pentasils" *Stud. Surf. Sc. and Cat.* **28**,633 (1986)

[27] R.M. Barrer in "Zeolites: Science and Technology" NATO ASI series E **80**, 227 Martinus Nijhoff Publications, The Hague (1984)